

Avoiding resonance capture in multi-planet extrasolar systems

Margaret Pan¹, Hilke E. Schlichting^{1,2}

ABSTRACT

A commonly noted feature of the population of multi-planet extrasolar systems is the rarity of planet pairs in low-order mean-motion resonances. We revisit the physics of resonance capture via convergent disk-driven migration. We point out that for planet spacings typical of stable configurations for *Kepler* systems, the planets can routinely maintain a small but nonzero eccentricity due to gravitational perturbations from their neighbors. Together with the upper limit on the migration rate needed for capture, the finite eccentricity can make resonance capture difficult or impossible in Sun-like systems for planets smaller than \sim Neptune-sized. This mass limit on efficient capture is broadly consistent with observed exoplanet pairs that have mass determinations: of pairs with the heavier planet exterior to the lighter planet — which would have been undergoing convergent migration in their disks — those in or nearly in resonance are much more likely to have total mass greater than two Neptune masses than to have smaller masses. The agreement suggests that the observed paucity of resonant pairs around sun-like stars may simply arise from a small resonance capture probability for lower-mass planets. Planet pairs that thereby avoid resonance capture are much less likely to collide in an eventual close approach than to simply migrate past one another to become a divergently migrating pair with the lighter planet exterior. For systems around M stars we expect resonant pairs to be much more common, since there the minimum mass threshold for efficient capture is about an Earth mass.

1. Introduction

In the last decade several hundred multiple-planet systems, together containing over 1300 planets, have been discovered, mostly through transit photometry surveys such as the *Kepler* mission. These systems comprise a statistically interesting sample of exoplanetary orbital configurations that can constrain the roles of different planet-planet interactions during system formation.

Of particular interest here is the occurrence of (near-)mean-motion resonances among planet pairs. Studies of the *Kepler* planet population indicate that these bodies are typically between Earth- and Neptune-sized and that typically \sim 1% of the planet mass lies in a hydrogen/helium envelope (see, for example, Wolfgang & Lopez 2015, and references therein). The presence of these light gases strongly suggests that these planets formed while their protoplanetary disks were still present. In the standard example of a minimum mass solar nebula (MMSN)-like disk, we expect

¹Massachusetts Institute of Technology, 77 Massachusetts Avenue, Cambridge, MA 02139

²University of California, Los Angeles, 595 Charles E. Young Drive East, Los Angeles, CA 90095

embedded planets to migrate inwards towards the star at speeds proportional to their masses. For Earth- to Jupiter-mass planets with very low eccentricities, pairs of planets undergoing convergent migration have an order unity chance of becoming locked in first-order resonances when their semimajor axis ratio reaches the relevant value. Nonetheless, a glance at the period ratios of adjacent planet pairs (pairs not known to have additional planets separating them) indicates that at most a few percent are currently likely to be in resonance (see Figure 1 and Fabrycky et al. 2014; Steffen & Hwang 2015). Pairs with period ratios just larger than several first-order mean motion resonance values do appear to occur more frequently than a smooth distribution would predict. This suggests that the nearby resonances may have significantly affected those pairs’ dynamics, and several groups have offered explanations for the observed offsets (see, for example, Lithwick & Wu 2012; Batygin & Morbidelli 2013; Baruteau & Papaloizou 2013; Petrovich et al. 2013; Delisle et al. 2014; Chatterjee & Ford 2015, and references therein).

However, even these near-resonant pairs are only $\sim 15\%$ of the total (see Figure 1), not enough to be consistent with the large nominal capture probability. To explain their rarity, several groups (see, for example, Adams et al. 2008; Rein & Papaloizou 2009) have proposed that turbulence may excite resonant planets’ random motions enough to disrupt the resonance. Goldreich & Schlichting (2014) and Delisle et al. (2014) proposed that pairs initially trapped in resonance might later escape due to overstable librations coupled with eccentricity damping. After escape, the planets would migrate away from resonance. On the other hand, Batygin (2015) proposed that the embedded planets’ eccentricities might be too large for efficient resonant capture to occur at all despite convergent migration. He finds $e \gtrsim 10^{-2}$ as the eccentricity criterion for efficient capture and notes that it is comparable to the typical Kepler planet eccentricity (Wu & Lithwick 2013; Hadden & Lithwick 2014). However, he does not address these finite eccentricities’ origin, or whether they occur during or after the time when the disk is present and migration is expected.

Here we discuss an explanation for why $e \gtrsim 10^{-2}$ may typically occur for many planets during disk migration: gravitational interactions between planets as they move through the disk. For smaller planets separated by several Hill spheres, close encounters between neighboring planets can excite eccentricities faster than planet-disk interactions can damp them. Combined with the requirement for efficient resonance capture that disk migration be slower than the resonant libration period, these finite eccentricities significantly limit the range of planet masses that can routinely capture into resonance. In §2 we define system parameters; in §3 we discuss timescales for migration and close encounters; in §4 we discuss the typical planet eccentricity; in §5 we discuss the implications for resonant capture in the context of the known multiplanet systems; and in §6 we summarize our findings.

2. Planetary system parameters

We assume a young solar system centered on a star of mass M_* , radius R_* , and bulk density ρ_* . The system contains a passively heated mostly gaseous circumstellar disk similar to the minimum mass solar nebula (MMSN). The disk has mass surface density $\sigma_g(a) \propto a^{-3/2}$ (where a is the semimajor axis); scale height $h_g \propto a^{5/4}$; and volume density $\rho_g \sim \sigma_g/h_g$. Embedded in the disk

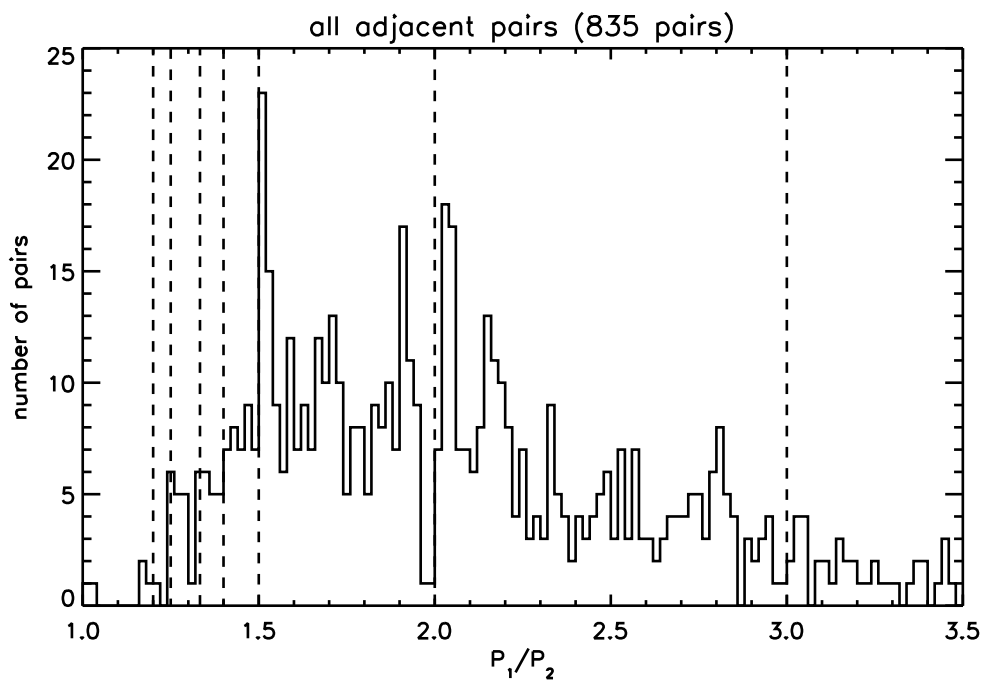


Fig. 1.— Period ratio histogram of all pairs of adjacent planets in the NASA Exoplanet Archive as of 2016 May 25. While peaks in the histogram occur just outside several mean motion resonances (dashed lines), most pairs seem to be completely unassociated with such resonances.

are young planets near the isolation mass (Lissauer 1987). Their orbital spacings are typically of order a few times their Hill spheres, $R_H \simeq \mu^{1/3}a$, where μ is the planet/star mass ratio, μM_* is the planet mass, and a is the planet semimajor axis. In discussions of rates of collision and resonant capture we focus on two planets of masses μM_* and $f^3 \mu M_*$ where f is a numeric constant; bulk density ρ ; and sizes R and fR . The planets orbit at semimajor axes a_1, a_2 and with eccentricities e_1, e_2 . We assume the planets are too small to open gaps in the disk. We also assume $\rho_* \simeq \rho$; for a late main-sequence star and typical planets, both are of order unity (g cm^{-3}).

For convenience, we define $\alpha = R_*/a$, so that the Hill radius becomes $R_H = \alpha^{-1}R$ and Hill velocity is $v_H = \alpha^{1/2}v_{\text{esc}} \simeq \alpha^{1/2}R\sqrt{G\rho}$. We also use the usual orbital angular frequency $\Omega \simeq \sqrt{G\rho}\alpha^{3/2}$, orbital velocity $v_K \simeq \Omega a$, and gas sound speed $c_g \simeq h_g\Omega$.

If migration is integral to planetary system architectures, we would expect planets currently at or inside $a = 1$ AU to have formed and interacted further out. For the sake of representative numerical estimates, unless otherwise noted, we assume a MMSN disk around a solar type star at a semimajor axis 10 AU. These parameters imply $\alpha \sim 0.0005$, $\sigma_g \sim 55 \text{ g cm}^{-2}$, $h_g/a \sim 0.18$, which we will refer to as “standard conditions”. They give an isolation planet mass of $\sim 4 \times 10^{27} \text{ g}$ (see, for example, Schlichting 2014).

3. Encounter timescales

3.1. Migration

Convergent disk-mediated migration is a natural mechanism for inducing planet pairs’ resonance crossings and possible capture. We briefly review migration caused by gas drag and by gravitational torques exerted by the disk on the planet.

Due to pressure support, the gas orbits slower than the local Keplerian velocity by a fraction

$$\frac{\delta v}{v_K} \sim \left(\frac{c_g}{v_K} \right)^2 . \quad (1)$$

As a result planets moving through the gas feel a drag force and drift towards the star at a rate

$$\frac{1}{a} \frac{da}{dt} \sim \frac{\sigma_g}{\rho R} \frac{h_g^3}{a^3} \Omega \sim \frac{\mu_d}{\mu^{1/3}} \alpha^2 \frac{h_g^3}{a^3} \Omega , \quad (2)$$

assuming they are in the Stokes regime. Here, $\mu_d \sim \sigma_g a^2 / M_*$ is the ratio of the stellar mass and the local disk mass, or the disk mass within a semimajor axis range of about a factor of two about a ; it does not represent the total disk mass. At the same time, gravitational interactions between a planet and nearby disk gas lead to torque exchange. In a circular disk where the density decreases sufficiently slowly outwards, and where the viscosity circularizes gas molecules’ trajectories within one synodic period, the asymmetry between interactions with interior and exterior gas is of order h_g/a , giving inward Type I migration rate

$$\frac{1}{a} \frac{da}{dt} \sim \frac{\mu^2}{(h_g/a)^5} \cdot \frac{\sigma_g h_g/a}{\rho R^3} \cdot \frac{h_g}{a} \cdot \frac{h_g}{a} \Omega \sim \mu \mu_d \left(\frac{a}{h_g} \right)^2 \Omega . \quad (3)$$

3.2. Encounter timescales

Two planets may capture into resonance only while their semimajor axis ratio differs from exact resonance by less than the (fractional) resonance width $\sim \mu^{2/3}$ (Murray & Dermott 1999). We take an encounter to last while the semimajor axes of the planets in question are within this range. If the planets are migrating due to disk interactions as described above, the time to cross this distance is

$$\mu^{2/3} \left(\frac{1}{a} \frac{da}{dt} \right)^{-1} \sim \begin{cases} \frac{\mu}{\mu_d} \frac{a^3}{h_g^3} \alpha^{-2} \frac{|1-f^{-1}|^{-1}}{\Omega} \propto a^{9/4} \mu^1 & \text{Stokes} \\ \frac{1}{\mu_d \mu^{1/3}} \left(\frac{h_g}{a} \right)^2 \frac{|1-f^3|^{-1}}{\Omega} \propto a^{3/2} \mu^{-1/3} & \text{Type I} \end{cases} \quad (4)$$

where μ is the larger of μ_1, μ_2 . Note the Stokes drag timescale increases while the Type I timescale decreases with increasing μ . The two inward migration rates match at

$$\mu \sim \alpha^{3/2} \left(\frac{h_g}{a} \right)^{15/4} \propto a^{-9/16} \quad , \quad (5)$$

which corresponds to an upper bound on the encounter time of

$$\sim \frac{1}{\mu_d} \alpha^{-1/2} \left(\frac{h_g}{a} \right)^{3/4} \frac{1}{\Omega} \propto a^{27/16} \quad . \quad (6)$$

For a MMSN around a solar type star at 10 AU, the slowest encounter takes $\sim 10^5$ yrs and occurs for $(\mu_1, \mu_2) \sim \mu \sim 10^{-8}$, or $R \sim 10^3$ km.

4. Typical eccentricities

Perhaps the physically simplest way to excite planets' eccentricities is gravitational perturbations from neighboring bodies. To find the typical eccentricity thus induced, we first calculate the gravitational stirring rate. We take the typical spacing between planets to be CR_H where $C \simeq 10$, following the multiplanet stability limit simulations of Pu & Wu (2015). Since planet formation theory also predicts spacings of \sim several R_H during oligarchy (see, for example, Goldreich et al. 2004, and references therein), we believe this is a reasonable estimate for planet separations. A close approach within R_H typically gives the planets an additional random velocity of v_H , or eccentricity $v_H/(\Omega a) \sim \mu^{1/3}$. Then bodies of mass μ spaced CR_H apart typically impart eccentricities $\sim \mu^{1/3} C^{-2}$ to one another during a single conjunction³.

This eccentricity is damped by disk interactions at a rate

$$\frac{1}{e} \frac{de}{dt} \sim \mu \mu_d \left(\frac{a}{h_g} \right)^4 \Omega \propto a^{-2} \mu^1 \quad (7)$$

³This approximation is reasonable as long as CR_H is significantly less than unity. E.g. with $C = 10$, this holds for planets significantly smaller than a Jupiter mass. For larger separations, it is a slight underestimate: at the separation of bodies in the 2:1 resonance, the inverse square scaling with distance gives an interaction too small by a factor of 1.4.

per Goldreich & Schlichting (2014). This is slower than the synodic frequency $\Omega CR_H/a$ as long as

$$\mu \lesssim C^{3/2} \mu_d^{-3/2} \left(\frac{h_g}{a} \right)^6, \quad (8)$$

which is easily satisfied for all the cases we consider here. This implies that the eccentricity gained at one conjunction will not be damped before the next conjunction. Since the planets are not in resonance, the longitudes of successive conjunctions are uncorrelated, and the planets' eccentricities increase per a random walk with steps of size $\sim \mu^{1/3} C^{-2}$ taken once every synodic time until an eccentricity damping time has elapsed. This yields

$$\text{typical eccentricity} \sim C^{-3/2} \mu_d^{-1/2} \left(\frac{h_g}{a} \right)^2. \quad (9)$$

Note that the typical eccentricity is independent of μ .

Finally, even if the typical separation is CR_H , planets migrating at different rates will occasionally pass one another, leading to a close approach within R_H . As we discuss in §5.2.3, direct collisions are unlikely during these close approaches. However, if the larger eccentricities attained at these $\lesssim R_H$ approaches persist at larger separations, they may dominate the typical excitation from stirring expressed in Equation 9. We therefore check whether eccentricities excited during these very close approaches can damp quickly as the neighboring planets differentially migrate away from each other. To do this we compare the eccentricity damping timescale to the time required to migrate through R_H :

$$\frac{\frac{1}{e} \frac{de}{dt} \Big|_{\text{damp}}}{\frac{1}{\mu^{1/3} a} \frac{da}{dt}} \sim \begin{cases} \mu^{5/3} \left(\frac{a}{h_g} \right)^7 \alpha^{-2} & \text{Stokes} \\ \mu^{1/3} \left(\frac{a}{h_g} \right)^2 & \text{Type I} \end{cases}. \quad (10)$$

Setting the above to unity and solving for μ , we find

$$\mu \gtrsim \begin{cases} \left(\frac{h_g}{a} \right)^6 \propto a^{3/2} & \text{Stokes} \\ \left(\frac{h_g}{a} \right)^{21/5} \alpha^{6/5} \propto a^{-3/20} & \text{Type I} \end{cases} \quad (11)$$

is required for damping to occur faster than migration through R_H . For our standard disk conditions, eccentricity damping occurs faster than migration through R_H only for planets larger than $\mu \sim 9 \times 10^{-7}$. For smaller planets down to the Type I-Stokes boundary, eccentricities of order e_{crit} persist as the planets migrate past nearest-neighbor separation R_H . Thus for planets larger than $\mu \sim (h_g/a)^{21/5} \alpha^{6/5}$, eccentricities are excited to $\gtrsim e_{\text{crit}}$ while their nearest neighbor planet orbit lies within R_H ; once they migrate away, their eccentricities settle to a new equilibrium set by more distant close approaches at $\sim CR_H$. Equation 9 accurately represents these planets' typical eccentricities. For smaller planets, eccentricities grow to $\gtrsim e_{\text{crit}}$ while the nearest neighbor planet orbit lies within R_H and do not damp quickly afterwards. For much of the time, these planets' eccentricities may be larger than that given by Equation 9.

5. Resonance capture

5.1. Chance of capture per encounter

Two convergently migrating planets may eventually reach orbital separations consistent with a $p : q$ mean-motion resonance, that is, a semi-major axis ratio closer to the exact resonance ratio $(p/q)^{2/3}$ than the fractional resonance width $\sim \mu^{2/3}$. To guarantee resonant capture during the planets' pass through this range, the time to cross the resonance must be longer than the critical libration timescale $\sim \mu^{-2/3} \Omega^{-1}$ (Goldreich & Schlichting 2014). This requires

$$\mu \gtrsim \begin{cases} \alpha^{6/5} \mu_d^{3/5} \left(\frac{h_g}{a}\right)^{9/5} \propto a^{-9/20} & \text{Stokes} \\ \mu_d^3 \left(\frac{a}{h_g}\right)^6 \propto a^{-1} & \text{Type I} \end{cases} . \quad (12)$$

However, this argument only makes sense if, despite conjunctions with nearby planets before an encounter, the eccentricities of the planets undergoing the encounter remain low enough to make capture likely. The eccentricity threshold for efficient resonance capture is $e_{\text{crit}} \sim \mu^{1/3}$ (Goldreich & Schlichting 2014), so planets whose typical eccentricity remains below e_{crit} should capture efficiently. Using Equation 9, these planets must have

$$\mu \gtrsim C^{-9/2} \mu_d^{-3/2} \left(\frac{h_g}{a}\right)^6 \propto a^{3/4} . \quad (13)$$

We would expect smaller planets to have typical eccentricity larger than $\mu^{2/3}$. At those higher eccentricities, capture is possible but less likely: the eccentricities of planets librating in resonance may oscillate through larger values, but in order for capture to occur at high eccentricities, the phases of the planets as they reach the resonance must match the phases where high eccentricities are attained. Using the Hamiltonian as in Murray & Dermott (1999), we calculate the capture probability to decrease as [eccentricity]^{-1.43}.

5.2. Resonant planet pairs

5.2.1. Sun-like stars

For solar system-like conditions, that is, $\mu_d \sim 10^{-3}$ at 10 AU, the numerical estimates in Sections 4 and 5.1 apply: planets with $\mu \gtrsim 3 \times 10^{-5}$ migrate slowly enough and maintain sufficiently small eccentricities to capture into resonance during a close encounter. For disk masses smaller than this, planet-planet scattering increases the eccentricities of all planets above e_{crit} before resonance entry, greatly decreasing the chance of capture. Occasional close approaches within R_H do not strongly affect the typical eccentricity for planets larger than $\mu \sim 8 \times 10^{-8}$. For larger disk masses, the smallest planet that migrates slowly enough to be captured increases as μ_d^3 until that planet becomes large enough to open a gap in the disk. Once this occurs, the planet becomes locked to the disk and its migration rate slows dramatically. The planet mass where this occurs depends on the

disk viscosity; as a representative value we take $\mu \sim 0.2(h_g/a)^3$ using Figure 6 of Rafikov (2002). The above results are summarized in the top panels of Figure 2.

The Kepler planet sample is in broad agreement with this estimate (Figures 3 and 4): among pairs of adjacent planets with the more massive planet outside — a configuration consistent with convergent migration in a MMSN-type disk — near-resonant pairs are much more likely to have combined mass >2 Neptune masses than to have lower masses. The 2:1, 3:2, and 4:3 resonances are associated with 18 higher mass pairs of combined mass $> 2M_{\text{Neptune}}$ vs. 6 lower mass pairs of combined mass $< 2M_{\text{Neptune}}$. Of those 6, one includes a planet of mass $1.2M_{\text{Neptune}}$ and one orbits an M dwarf. At the same time, the period distribution shapes in the top (lighter planet exterior) and bottom (heavier planet exterior) panels of Figure 3 differ qualitatively: the near-resonance peaks appear much more pronounced in the bottom than in the top panel. This supports the idea that convergent migration leading to resonance capture does occur among exoplanets.

5.2.2. *M stars*

Because \sim Earth-sized planets in the habitable zones of M stars produce deeper transits more frequently than their analogues orbiting solar-type stars, interest in M star planetary systems continues to grow. An early- to mid-M main-sequence star might have $M_* = M_{\odot}/5$, $R = R_{\odot}/2$, planets near $a = 0.1$ AU, and a disk mass of $0.01M_*$ spread between 0.01 AU and 5 AU. As with the sun-like systems, we assume the planets formed and interacted further out, so we consider the dynamics at 1 AU. With $\sigma_g \propto a^{-3/2}$, we have $\alpha \sim 0.0025$, $\sigma_g \sim 3.3 \times 10^2$, and $h_g/a \sim 0.13$. Results for these system parameters are summarized in the bottom panels of Figure 2: we expect M dwarf planets in the Earth- to super-Earth size range and larger to be able to capture efficiently into resonance. Although the number of M dwarf systems with measured planet masses is currently too small to provide meaningful statistical contrast with the sample of FGK systems, we would expect future surveys such as the *TESS* mission to show similar period ratio distributions roughly independent of planet mass. Nonetheless, systems such as TRAPPIST-1, with seven planets all below $1.5M_{\text{Earth}}$ in resonances (Gillon et al. 2017), and Kepler-32, with three out of five planets near mean-motion resonances and smaller than 0.6 Neptune radii (Fabrycky et al. 2012), appear broadly consistent with our prediction.

5.2.3. *Location of resonant encounters and close approaches*

In the above discussions we assumed the resonant interactions occurred at significantly larger semimajor axes than those common in known multiplanet systems. Taking the resonant encounters to have occurred at the planets' current locations instead would require migration to have stopped immediately post-encounter, and we have no reason to expect such fine-tuned agreement between the disk lifetime and the time of the encounter. However, from Equations 12 and 13, the minimum

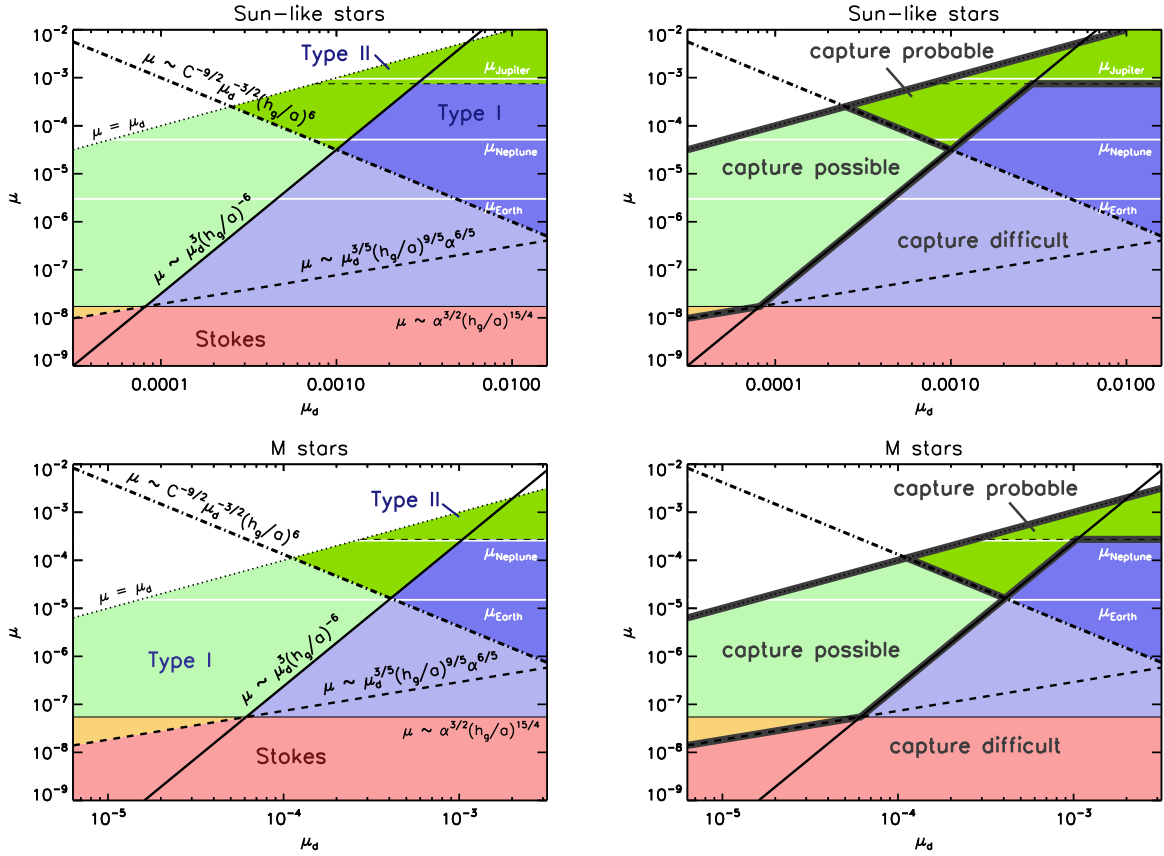


Fig. 2.— Summary plots showing areas of likely resonant capture (bright green), possible resonant capture (light green, orange), and unlikely resonant capture (blue, red) as a function of planet mass ratio μ and disk mass ratio μ_d . Left and right hand columns show the same results, but plots in the right column emphasize regions corresponding to different resonant encounter outcomes. Top panel assumes a star of mass M_\odot and radius R_\odot , semimajor axis 10 AU, and disk scale height $h_g/a = 0.1(a/1\text{AU})^{1/4}$; bottom panel assumes a star of mass $M_\odot/4$ and radius $R_\odot/2$, semimajor axis 1 AU, and disk scale height $h_g/a = 0.1(a/0.4\text{AU})^{1/4}$. In red/orange regions, migration by Stokes drag dominates; in blue/green regions, Type I migration is faster. The most massive planets (above the thin dashed line; numbers from Figure 6 of Rafikov (2002) assuming disk α -parameter $\sim 10^{-5}$) open gaps in their disks, slowing their migration dramatically. In regions of unlikely resonant capture, the time for migration across a resonance width is faster than the libration period. In regions of likely capture, migration is sufficiently slow and typical eccentricities are sufficiently small for efficient capture. In regions of possible capture, migration is sufficiently slow but eccentricities are larger than the threshold value $\sim \mu^{1/3}$; here the probability of capture decreases approximately as [eccentricity] $^{-1.43}$. Since it is unrealistic for the planets to be more massive than their disk at this stage, all regions are cut off at $\mu = \mu_d$. For sun-like systems, only planets more massive than about a Neptune mass are likely to be captured. For M dwarf systems, planets larger than about half an Earth mass are likely to be captured. In both cases a sufficiently massive disk is required; for sun-like systems the lower limit for efficient capture is close to the MMSN, and for M dwarf systems it is close to a $0.01M_*$ disk covering the range 0.01 to 5 AU with $\sigma_g \propto a^{-3/2}$.

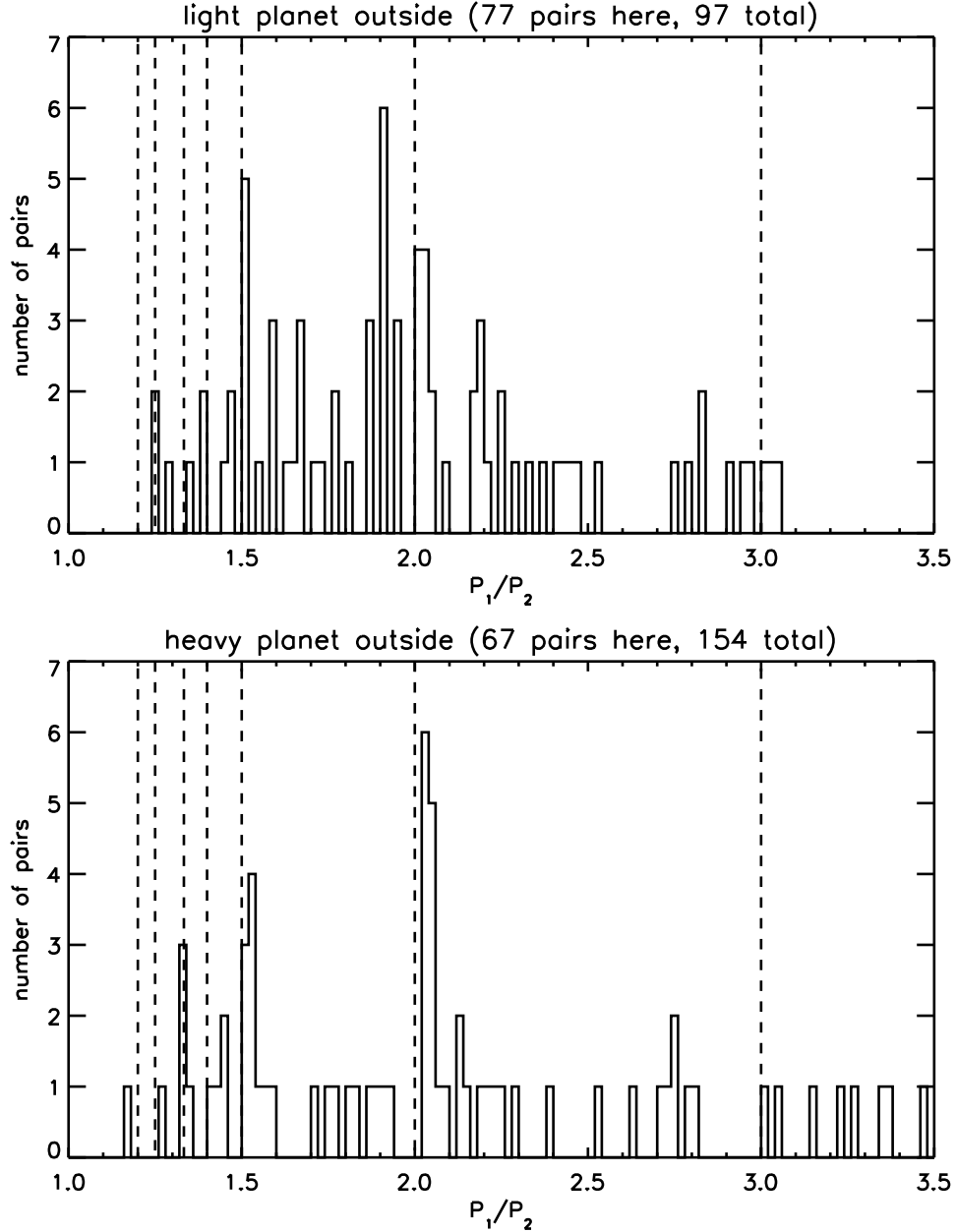


Fig. 3.— Histograms of orbit period ratios for pairs of adjacent Kepler planets (pairs not known to have additional planets between them) in multi-planet systems with measured masses as of 2016 May 25. Mean-motion resonance locations are indicated by dashed lines. When the outer planet is the more massive of the pair (bottom panel), the peaks near resonances are much more pronounced than when the outer planet is the less massive (top panel). Since convergent migration in a MMSN-type disk occurs only when the more massive planet is exterior, this supports the idea that migration indeed pushes planet pairs into resonance.

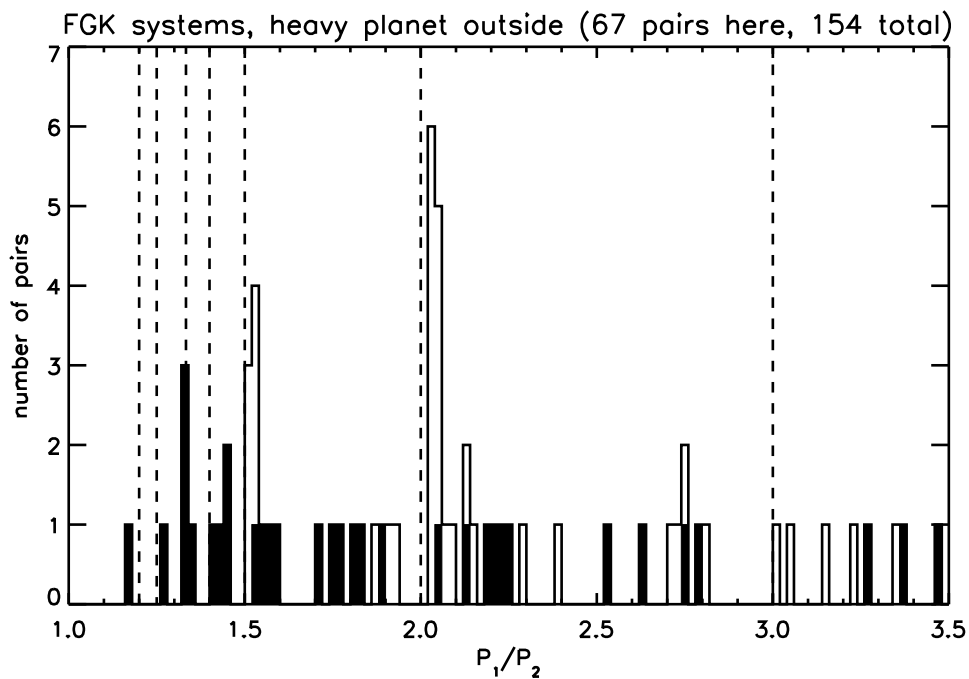


Fig. 4.— Similar to the bottom panel of Figure 3 except that while the unshaded histogram includes all such pairs, the shaded histogram includes all pairs with combined mass less than $0.1M_{\text{Jupiter}} \simeq 2M_{\text{Neptune}}$. That the vast majority of near-resonant pairs occur among systems with combined planet mass $> 2M_{\text{Neptune}}$ supports our estimates in Section 5.2.

planet mass that efficiently captures into resonance⁴,

$$\mu_{\min} \sim C^{-3} \left(\frac{h_g}{a} \right)^2 \propto a^{1/2} \quad , \quad (14)$$

decreases with decreasing semimajor axis. For example, taking our usual MMSN-like system parameters at 1 AU with $C = 10$ gives $\mu_{\min} \sim 10^{-5}$, equivalent to $\sim 3M_{\text{Earth}}$, rather than the $\mu_{\min} \sim 3 \times 10^{-5}$ we find at 10 AU. The reasonable agreement between our numbers (Figure 2) and observed systems (Figure 4) suggests that most resonant encounters occurred in disks with μ_d and h_g/a similar to those of our standard conditions. In a MMSN-like system, this implies semimajor axis values beyond the ice line. Planet pairs that failed to capture into resonance via convergent migration at those larger semimajor axes would eventually have a close approach, stir one another, and continue inwards, most likely migrating divergently. Planet-planet collisions during these close passages are unlikely: the chance of collision is roughly the collision probability per conjunction times the number of conjunctions that occur as the planets migrate through their mutual Hill sphere,

$$\alpha \cdot \frac{\mu^{2/3} \mu_d \frac{a^2}{h_g^2} \Omega}{\mu^{1/3} \Omega} \sim \mu^{1/3} \mu_d \left(\frac{a}{h_g} \right)^2 \alpha \propto \mu^{1/3} a^{-1} \quad , \quad (15)$$

where we applied Equation 3. Here we assumed that the planets undergo Type I migration and that their random velocities are $\sim v_H$, since it takes just a few conjunctions within R_H for them to stir each other’s velocities to this level (Goldreich et al. 2004). With our standard disk parameters and planets of ~ 5 Earth masses, the chance of collision is $\sim 10^{-7}$. This suggests that many pairs that today have the lighter planet exterior could have originally been convergently migrating with the heavier planet exterior.

Finally, when $([(p+1)/p]^{2/3} - 1)\mu^{-1/3} \lesssim 10$, the spacing between two planets at the $p+1 : p$ resonance is such that $C < 10$. Since resonance capture would for these larger planets require a nearest neighbor closer than $C = 10$, we would expect them to acquire eccentricities larger than that given by Equation 9 with $C = 10$ just before arriving at the resonance. In general a closer spacing makes resonance capture more difficult: if the typical spacing were $C < 10$ the μ_{\min} of Equation 14 would increase, making resonant capture of low-mass planets even more unlikely. However, we see from Equation 14 that even Jupiter mass planets around sun-like stars ($\mu_{\text{Jupiter}} \simeq 9.5 \times 10^{-4}$) at 10 AU lie above μ_{\min} for the 2:1 and 3:2 resonances, and this condition only becomes easier to satisfy closer to the star. Thus the smaller C does not preclude resonance capture for large planets.

6. Summary

Given a population of young planets embedded in a protoplanetary disk, we derived a typical planet eccentricity as a function of planet mass by comparing the rates of eccentricity excitation

⁴As is true in the sun-like and M star systems discussed here, we assume planets subject to efficient resonance capture are in the Type I regime.

due to stirring from nearby planets and eccentricity damping by the disk. We combined this with disk migration rate calculations to show that in systems similar to the early solar system, only planets \sim Neptune-sized or larger are likely to both migrate slowly enough and have eccentricities small enough for efficient capture into first-order resonance. This appears broadly consistent with observational data on multiplanet systems, which show that for planet pairs with a heavier exterior planet, the majority of those in or near first-order resonance have total mass $\gtrsim 2M_{\text{Neptune}}$. The agreement suggests the observed rarity of resonant pairs around sun-like stars may arise simply because it is too difficult for planets less massive than $\sim M_{\text{Neptune}}$ to capture into resonance in the first place. Likewise, our results support a scenario where formation and resonant interactions of many members of the known multiple exoplanet systems occurred outside the ice line. We expect many pairs that fail to capture into resonance to continue convergent migration, pass one another, and begin divergent migration: we find direct collisions should be rare in close approaches between planets. A significant fraction of pairs with the lighter planet exterior could therefore have originally been convergently migrating. For systems around M stars, we predict that a higher fraction of planet pairs will be resonant, as the lower mass limit for efficient resonance capture decreases to $\sim M_{\text{Earth}}$.

Ongoing and future planet searches such as HAT, K2, KELT, SPECULOOS, and TESS will greatly increase the population of known multiplanet systems and the range of host stellar types, providing an excellent sample with which to confront and refine our theory.

Acknowledgments. We gratefully acknowledge support from NASA grants NNX15AK23G and NNX15AM35G. We thank Re'em Sari for pointing out Rafikov's work on planet-disk torques and gap opening. This research has made use of the NASA Exoplanet Archive, which is operated by the California Institute of Technology under contract with the National Aeronautics and Space Administration under the Exoplanet Exploration Program. The final stages of writing took place partially at the Aspen Center for Physics, which is supported by NSF grant PHY-1066293.

REFERENCES

- Adams, F. C., Laughlin, G., & Bloch, A. M. 2008, ApJ, 683, 1117
- Baruteau, C., & Papaloizou, J. C. B. 2013, ApJ, 778, 7
- Batygin, K. 2015, MNRAS, 451, 2589
- Batygin, K., & Morbidelli, A. 2013, AJ, 145, 1
- Chatterjee, S., & Ford, E. B. 2015, ApJ, 803, 33
- Delisle, J.-B., Laskar, J., & Correia, A. C. M. 2014, A&A, 566, A137
- Fabrycky, D. C., Ford, E. B., Steffen, J. H., Rowe, J. F., Carter, J. A., Moorhead, A. V., Batalha, N. M., Borucki, W. J., Bryson, S., Buchhave, L. A., Christiansen, J. L., Ciardi, D. R., Cochran, W. D., Endl, M., Fanelli, M. N., Fischer, D., Fressin, F., Geary, J., Haas, M. R.,

- Hall, J. R., Holman, M. J., Jenkins, J. M., Koch, D. G., Latham, D. W., Li, J., Lissauer, J. J., Lucas, P., Marcy, G. W., Mazeh, T., McCauliff, S., Quinn, S., Ragozzine, D., Sasselov, D., & Shporer, A. 2012, *ApJ*, 750, 114
- Fabrycky, D. C., Lissauer, J. J., Ragozzine, D., Rowe, J. F., Steffen, J. H., Agol, E., Barclay, T., Batalha, N., Borucki, W., Ciardi, D. R., Ford, E. B., Gautier, T. N., Geary, J. C., Holman, M. J., Jenkins, J. M., Li, J., Morehead, R. C., Morris, R. L., Shporer, A., Smith, J. C., Still, M., & Van Cleve, J. 2014, *ApJ*, 790, 146
- Gillon, M., Triaud, A. H. M. J., Demory, B.-O., Jehin, E., Agol, E., Deck, K. M., Lederer, S. M., de Wit, J., Burdanov, A., Ingalls, J. G., Bolmont, E., Leconte, J., Raymond, S. N., Selsis, F., Turbet, M., Barkaoui, K., Burgasser, A., Burleigh, M. R., Carey, S. J., Chaushev, A., Copperwheat, C. M., Delrez, L., Fernandes, C. S., Holdsworth, D. L., Kotze, E. J., Van Grootel, V., Almléaky, Y., Benkhaldoun, Z., Magain, P., & Queloz, D. 2017, *Nature*, 542, 456
- Goldreich, P., Lithwick, Y., & Sari, R. 2004, *ARA&A*, 42, 549
- Goldreich, P., & Schlichting, H. E. 2014, *AJ*, 147, 32
- Hadden, S., & Lithwick, Y. 2014, *ApJ*, 787, 80
- Lissauer, J. J. 1987, *Icarus*, 69, 249
- Lithwick, Y., & Wu, Y. 2012, *ApJ*, 756, L11
- Murray, C. D., & Dermott, S. F. 1999, *Solar system dynamics*
- Petrovich, C., Malhotra, R., & Tremaine, S. 2013, *ApJ*, 770, 24
- Pu, B., & Wu, Y. 2015, *ApJ*, 807, 44
- Rafikov, R. R. 2002, *ApJ*, 572, 566
- Rein, H., & Papaloizou, J. C. B. 2009, *A&A*, 497, 595
- Schlichting, H. E. 2014, *ApJ*, 795, L15
- Steffen, J. H., & Hwang, J. A. 2015, *MNRAS*, 448, 1956
- Wolfgang, A., & Lopez, E. 2015, *ApJ*, 806, 183
- Wu, Y., & Lithwick, Y. 2013, *ApJ*, 772, 74